2018 IEEE International Conference on Systems, Man, and Cybernetics

A Miniature Multi-Sensor Shoe-Mounted Platform for Accurate Positioning

Pooya Merat*, Edward J. Harvey†, Georgios D. Mitsis‡
*Electrical Engineering, McGill University, Montreal, Canada
† Division of Orthopedic Surgery, McGill University, Montreal, Canada
‡ Bioengineering Department, McGill University, Montreal, Canada

***Abstract*—In this work a miniature low-cost and low-power platform for foot-mounted navigation and foot clearance estimation is presented. The developed system includes an inertial measurement unit (IMU) and three accurate distance sensors. The distance sensors enable reliable foot clearance monitoring that additionally increases the accuracy of horizontal localization. The device can be easily clipped onto the user's shoe for easy data collection by means of fast data logging, Bluetooth communication, USB connection as well as a computer interface. We present the device hardware and sensor fusion formulations along with the test results and estimation of the measurement quality with and without proximity sensors.**

I. INTRODUCTION

Thanks to advances in micro-electromechanical systems (MEMS) technology, motion sensors are integrated into almost every wearable electronic device. The motion data acquired from these devices can be used for motion analysis, activity monitoring, rehabilitation [1], human-computer interaction systems, gaming, animation or pedestrian navigation [2].

Foot-mounted IMU has drawn a significant attention in the past decades for motion analysis. Foot is a very strategic location for IMU for the following reasons:

1) Convenience: Similar to the wrist, the foot is one of the most convenient places to attach a sensor without interfering with our everyday activities. A foot wearable device can be integrated as an addition to the common footwear in the form of an insole or a clip on device.
2) Gait signature: Being one of human body extremities, the foot is involved in most physical activities including sports and walking. Also gait, which is one of the unique characteristics of every individual is reflected on foot motion. Many neurological disabilities affect gait such as Parkinson's disease, cerebral palsy, semi-paraplegia and stroke. Also natural aging or fatigue could result in dangerous gait which is reflected on foot motion.
3) Zero velocity updating for inertial navigation: Since foot is frequently in contact with the ground (and becomes stationary) in most activities, in the contact period the accumulated errors can be canceled resulting in more robust measurements.
4) Potential for energy harvesting: For accurate measurement, the motion data needs to be sampled at high rate and processed on the device. Also eventually the processed information should be ideally transferred to the user in real-time or at important events through RF communication. The power consumption for such configuration with the current technology on a small battery would last only a few hours. On the other hand, foot is one of the most potent locations for high power energy harvesting during normal walking. This is because at each step foot both undergoes high acceleration and when it lands, large forces are applied to the ground. Both of these forces can be utilized for energy harvesting. Depending on the design of energy harvester, up to several watts of power can be harvested during normal walking. Such system could be integrated in the shoe, or as an add-on to the foot.

IMU-based navigation systems rely on inertial property and thus are not sensitive to the environment. However, low-cost MEMS IMUs have limited accuracy and IMU positioning is based on double integration and significant errors accumulate over time. To compensate for these errors, fusion with complementary information is necessary. For example, zero velocity update (ZVU) is a valid assumption in most cases when the foot is in contact with the floor and becomes stationary [3]. At the stationary periods, the velocity can be reset to zero in KF.

Recently [4], [5] have used proximity sensors to calculate the distance of the foot mounted sensor to the walking floor. The sensor reading is a function of the orientation of the sensor and foot height. Estimating the orientation using an IMU, the foot height can be estimated. Such a measurement can be integrated to a ZVU-aided INS to improve the localization accuracy. On the other hand, because direct distance readings are available, foot clearance can be estimated directly.

In the current work an easy to use and powerful testbed is designed for accurate foot positioning with an emphasis on compensating for vertical errors. The distance sensors operate based on time-of-flight and thus are insensitive to environment lighting and reflectance. The system is designed to be attached to any shoe as a clip-on for ease of use and data collection.

II. SYSTEM DESIGN

In this study, the designed hardware is optimized for flexibility, size and cost. The device consists of a microcontroller unit (MCU), an inertial measurement unit (IMU), three laser ranging sensors and a 4-in-1 barometer module. A powerful ARM-M7 Cortex with FPU microcontroller enables on-board processing for advanced sensor fusion and high speed logging

2577-1655/18/$31.00 ©2018 IEEE
DOI 10.1109/SMC.2018.00473

TABLE I
COST OF THE DEVICE

Component	Cost (CAD)[1]
PCB and assembly	5
microcontroller	10
IMU	5
Barometer	10[2]
SD Card	10[2]
Bluetooth	10[2]
Other components	5
Total	20 (50[3])

[1] Per board, for 1000 devices (as of Feb 2018, ca.mouser.com)
[2] Optional components
[3] Total price including all the optional components

on an SD card which yields long term and high throughput logging of processed and/or raw data for off-line analysis. High speed USB connectivity is used for fast transfer of logged data to computer for post processing. A computer GUI (through USB) as well as a mobile application (via BLE) are used for controlling and monitoring the state of the system. The power is supplied through a $300mAh$ lithium polymer battery. The device was designed to be compact as a wearable device; the dimensions of the device are $32 \times 20 \times 10mm$. A 3D printed case was used to encapsulate the device and protect the electronics from physical damage. The device is shown in Fig. 1. The detailed cost of the device can be seen in Table I.

Fig. 1. The Developed System

Three VL53L0X sensor module is used for distance measurement. It is an infrared (940nm IR) time-of-flight (ToF) laser-ranging sensor made by STMicroelectronics. It operates based on measurement of the time that an emitted signal takes to travel to the target and reflect back. Using the speed of light the distance can be calculated. The device integrates a vertical cavity surface-emitting laser (VCSEL) for emission and an array of single photon avalanche diodes (SPAD) for detection of the transmitted IR signal. Due to the logic of operation, the sensor readings are insensitive to target reflectance unlike conventional technologies. VL53L0X can provide absolute distance measurement of up to $2m$ with an accuracy of $1cm$.

The device performs oversampling to compensate for errors and increase the resolution before providing the measurement result. For this reason, the frequency of the device is limited to 50Hz. The lower the frequency, the higher the accuracy of the measurements. The measurement duration depends on the noise and certainty of measurement, as a result the output frequency is not constant and depends on the measurement condition.

In our implementation, the default output frequency, i.e. 33Hz is used. This means that the device reading will timeout at 30ms, whether a valid measurement is available or not (in case of no nearby target for example). The measurement status is indicated in the internal status register.

One of the very useful features of this module is the support for multi-sensor integration. This means that multiple sensors can be used pointing to the same target. Each sensor module has its unique signal transmission in order to avoid interference with other sensors of the same type. In our system three sensors are used to increase the effective sampling frequency and measurement accuracy.

The sensors are calibrated at each system startup, using the integrated ad hoc calibration performed in the device. For more information, see the VL53L0X datasheet at *http://www.st.com/resource/en/datasheet/vl53l0x.pdf*.

III. ALGORITHM

A. IMU Initial Calibration

Sensor calibration without special calibration equipment is a common practice [6], [7], [8], [9]. Here we have used a 3D printed icosahedron (a polyhedron with 20 triangular faces) for IMU calibration. The system (or each IMU sensor) is placed inside the icosahedron and after the IMU is stationary, the sensor readings are averaged and captured. Once the data is captured, the system signals the user to rotate the icosahedron to a new face. The icosahedron is designed so that there is a pointer on each side showing the direction where the icosahedron needs to be rotated, so the user does not need to keep track of faces. Also, the system rejects similar readings to avoid capturing data on repetitive faces in case of user error.

1) Gyroscopes: In our system the gyroscopes are only corrected for bias which is calculated by averaging the signal at each icosahedron face.

2) Accelerometers: The fifteen-parameter calibration for accelerometers performs corrections on sensitivity (or scale factor), misalignment, cross axis sensitivity and bias.

The sensor output can be modeled as:

$$Y = KLU + (K_T U + B_T)T + B + w \tag{1}$$

where Y is the 3×1 sensor reading, U is the 3×1 physical signal. K is the scale factor correction matrix, L is the cross axis and misalignment matrix and B is the bias defined as:

$$L = \begin{bmatrix} 1 & l_{xy} & l_{xz} \\ 0 & 1 & l_{yz} \\ 0 & 0 & 1 \end{bmatrix}, \quad K = \begin{bmatrix} k_x & 0 & 0 \\ 0 & k_y & 0 \\ 0 & 0 & k_z \end{bmatrix}, \quad B = \begin{bmatrix} b_x \\ b_y \\ b_z \end{bmatrix} \tag{2}$$

K_T and B_T are the temperature gain of scale factor and bias respectively and are defined as:

$$K_T = \begin{bmatrix} \eta_x & 0 & 0 \\ 0 & \eta_y & 0 \\ 0 & 0 & \eta_z \end{bmatrix}, \quad B_T = \begin{bmatrix} \psi_x \\ \psi_y \\ \psi_z \end{bmatrix} \tag{3}$$

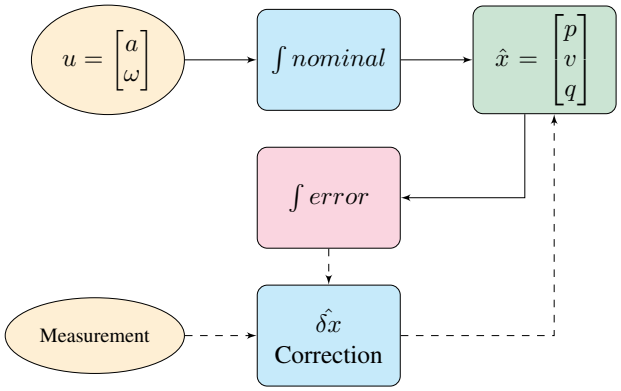

Fig. 2. IMU Error-Based Kalman Filter

Together K, L, K_T, B_T and B make up the 15 parameters of the accelerometer sensor model.

The captured sensor readings during calibration is fit to the equation model 1 using a trust region reflective algorithm which is performed on the on-board MCU.

B. IMU Fusion with Error-State Kalman Filter

We use an error-state Kalman filter (ESKF) for fusing the information. The general structure of the filter is well explained in [10]. In ESKF, instead of the system states, the deviation of integrated state from the true state is estimated. The algorithm is depicted in Fig. III-B.

The system input accelerometer and gyroscope readings is defined as $u = [a, \omega]$ and the system state including position $p_{3\times1}$, velocity $v_{3\times1}$ and orientation ($q_{4\times1}$ or $R_{3\times3}$) as $\hat{x} = [p, v, q]$. The error state δx is the deviation of $\hat{x}$ from the true state and i is the perturbation impulses defined as:

$$x_{4\times1} = \begin{bmatrix} p \\ v \\ q \end{bmatrix}, \quad \delta x_{3\times1} = \begin{bmatrix} \delta p \\ \delta v \\ \delta\theta \end{bmatrix}, \quad u = \begin{bmatrix} a \\ \omega \end{bmatrix}, \quad i = \begin{bmatrix} v_i \\ \theta_i \end{bmatrix} \tag{4}$$

$\delta\theta$ is the orientation error represented in *angle-axis* notation in the fixed global coordinate frame. The state space evolution of the nominal state can be represented as:

$$\begin{aligned} \Delta v &= (R(a) - g)\Delta t \\ p &\leftarrow p + v\Delta t + \frac{1}{2}\Delta v \Delta t \\ v &\leftarrow v + \Delta v \\ q &\leftarrow q \otimes q\{\omega\Delta t\} \end{aligned} \tag{5}$$

where g is the gravity vector, p is the 3D position vector, v is the 3D velocity vector in global frame. q is the 4D unit quaternion representation of local navigation frame in global frame. The $q\{\vec{\vartheta}\}$ is the quaternion unit vector corresponding to the rotation vector $\vec{\vartheta}$ in *angle-axis* representation and is:

$$q\{\vec{\vartheta}\} = \begin{bmatrix} \cos(\frac{\vec{\vartheta}}{2|\vartheta|}) \\ |\vartheta| \sin(\frac{\vec{\vartheta}}{2|\vartheta|}) \end{bmatrix} \tag{6}$$

where $|\vartheta|$ is the euclidean norm of ϑ. The error state evolution equations are:

$$\begin{aligned} \delta p &\leftarrow \delta p + \delta v \Delta t \\ \delta v &\leftarrow \delta v - [R(a)]_\times \delta\theta\Delta t + v_i \\ \delta\theta &\leftarrow R^T\{\omega\Delta t\}\delta\theta + \theta_i \end{aligned} \tag{7}$$

where v_i and θ_i are the velocity and orientation perturbations impulses respectively and are considered Gaussian with zero mean:

$$\begin{aligned} v_i &\sim N\{0, V_i\} \\ \theta_i &\sim N\{0, \Theta_i\} \end{aligned} \tag{8}$$

and with covariance matrices of v_i and θ_i respectively, and assuming that accelerometer and gyroscope noise is isotropic:

$$\begin{aligned} V_i &= \sigma_{a_n}^2 \Delta t^2 I \\ \Theta_i &= \sigma_{w_n}^2 \Delta t^2 I \end{aligned} \tag{9}$$

The complete error state system will become:

$$\delta x = F_x(x, u)\delta x + F_i.i \tag{10}$$

where F_i is the process noise matrix and is calculated as equation 12. The error prediction system is:

$$\begin{aligned} \hat{\delta x} &\leftarrow F_x \hat{\delta x} \\ P &\leftarrow F_x P F_x^T + F_i Q_i F_i^T \\ \delta x &\sim N\{\hat{\delta x}, P\} \end{aligned} \tag{11}$$

By comparing them to equations 7 and 13 we have:

$$\begin{aligned} F_x(x, u) &= \begin{bmatrix} I & I\Delta t & 0 \\ 0 & I & -[R(a)]_\times \Delta t \\ 0 & 0 & I \end{bmatrix}, \\ F_i &= \begin{bmatrix} 0 & 0 \\ I & 0 \\ 0 & I \end{bmatrix}, \quad Q_i = \begin{bmatrix} V_i & 0 \\ 0 & \Theta_i \end{bmatrix} \end{aligned} \tag{12}$$

C. Complementary Sensor Fusion

The complementary sensor data must be a function of true state:

$$\begin{aligned} y &= h(x) + \eta \\ \eta &\sim N\{0, R\} \end{aligned} \tag{13}$$

where η is the measurement noise and R is its covariance. The measurement update equations are:

$$\begin{aligned} K &= PH^T(HPH^T + R) \\ \hat{\delta x} &= K(y - h(\hat{x})) \\ P &= (I - KH)P \\ R_i &\sim N(0, R_i) \end{aligned} \tag{14}$$

H is the Jacobian matrix of $h(x)$ with respect to error state δx which can be written as:

$$\begin{aligned} H &\triangleq \frac{\partial h}{\partial \delta x}\Big|_x = \frac{\partial h}{\partial x_t}\Big|_x \frac{\partial x_t}{\partial \delta x}\Big|_x = H_x X_{\delta x} \\ X_{\delta x} &\triangleq \begin{bmatrix} I_6 & 0_{6\times 3} \\ 0_{4\times 6} & Q_{\delta\theta} \end{bmatrix} \\ Q_{\delta\theta} &= \frac{1}{2}\begin{bmatrix} -q_x & -q_y & -q_z \\ q_w & q_z & -q_y \\ -q_z & q_w & q_x \\ q_y & -q_x & q_w \end{bmatrix} \end{aligned} \tag{15}$$

where H_x is the momentary transformation matrix of nominal states to measurement. The transformed measurement is injected to correct the estimate of nominal states (i.e. $x \leftarrow x \oplus \hat{\delta x}$):

$$\begin{aligned} p &\leftarrow p + \delta p \\ v &\leftarrow v + \delta v \\ q &\leftarrow q\{\hat{\delta\theta}\} \otimes q \end{aligned} \tag{16}$$

The next step would be to reset the error state to zero and update the covariance matrix according to new error state:

$$\begin{aligned} \hat{\delta x} &\leftarrow 0 \\ P &\leftarrow GPG^T \\ G &= \begin{bmatrix} I_6 & 0 \\ 0 & I_3 + \left[\frac{1}{2}\hat{\delta\theta}\right]_\times \end{bmatrix} \end{aligned} \tag{17}$$

1) Zero Velocity Fusion: During ZVU period we assume that the velocity vector is 0, thus the measurement y_v would be:

$$\begin{aligned} y_v &= 0 + \eta_v \\ \eta_v &\sim N\{0, R_v\} \end{aligned} \tag{18}$$

The measurement noise covariance R_v and transformation H_v would become:

$$\begin{aligned} R_v &= \sigma_v^2 I_3 \\ H_v &= \begin{bmatrix} 0_3 & I_3 & 0_3 \end{bmatrix} \end{aligned} \tag{19}$$

Replacing H with H_v and R with R_v in equations 14 will complete ZVU formulation.

2) Foot Height Fusion: A single point time-of-flight (ToF) proximity sensor, measures the line-of-sight distance to the pointing target. Since it is based on time, theoretically it should be independent of environment lighting and color and reflectance of the target. The accuracy of the ToF is discussed in [11] with respect to color and dynamic motion of the target.

In this work we have used three ToF sensors placed parallel to each other facing the same side. The reason for having several distance sensors was to increase the resultant output frequency and accuracy of the whole system. In this section we assume the floor is flat and the system does not move relative to foot over time.

The distance reading represents a 3D vector in global coordinates. Knowing the orientation of the device and the distance sensor reading, this vector can be calculated and its

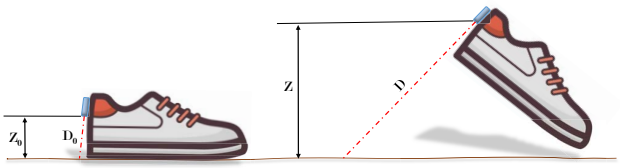

Fig. 3. Sensor reading to foot height correlation

z component of would be the height of the device from the floor (Fig. 3):

$$\begin{aligned} y_z &= -[0\ 0\ 1]R((d+\eta_d).u_d + r) \\ \eta_d &\sim N\{0, \sigma_d^2\} \end{aligned} \tag{20}$$

where z is the estimated foot vertical distance to ground, R is the estimated local to global rotation matrix, r the location of ToF sensor with respect to IMU in local frame, u_d is the unit vector of ToF sensor direction in the local frame, d is the sensor reading and σ_d^2 is the variance of d. The measurement noise covariance R_d and transformation H_d would become:

$$\begin{aligned} R_z &= \sigma_z^2 \\ H_z &= \begin{bmatrix} 0\ 0\ 1\ 0\ 0\ 0\ 0\ 0\ 0 \end{bmatrix} \end{aligned} \tag{21}$$

Replacing H with H_z and R with R_z in equations 14 completes the foot height fusion formulation.

3) Zero Velocity Detection: Zero velocity for foot mounted IMUs is defined at the instance when the sensor is almost stationary which occurs in normal gait during the stance phase. The trivial solutions involve looking at accelerometer and gyroscope signals over a recent time window and if they meet certain criteria, the IMU is deemed to be stationary [12]. The general criteria can be formulated as:

$$\begin{aligned} \frac{1}{W}\sum_{k=i}^{i+W-1} f_a(a_k) &< \gamma_a \\ \frac{1}{W}\sum_{k=i}^{i+W-1} f_\omega(\omega_k) &< \gamma_\omega \end{aligned} \tag{22}$$

where a_k and ω_k are accelerometer and gyroscope readings respectively. Sensor readings are summed over W number of samples. f_a and f_ω are some test functions and γ_a and γ_ω are some threshold values. The designer can decide if the IMU is stationary when one or both of the criteria are met.

Since during a zero velocity period the KF states are reset, the performance of positioning is very sensitive to selection of the parameters. Nevertheless, the performance may not be consistent between different speeds of walking among different people. Other type of sensors can be used to make ZVU detection more robust such as force sensing under the foot [12]. However it requires placement of sensors under the foot-wearable which may not be always feasible.

In this work we use the ToF distance readings in addition to monitoring the angular rate. In this configuration, we consider

the system stationary if both of the following conditions are met:

$$\frac{1}{W}\sum_{k=i}^{i+W-1}|\omega_k| < \gamma_\omega \tag{23}$$

$$\frac{1}{W}\sum_{k=i}^{i+W-1}(Z_k - Z_0) < \gamma_z \tag{24}$$

Equation 23 is a form of equation 22 where $f_\omega = |\omega_k|$ is the magnitude of angular rate. In equation 24, Z_k is the foot height estimation by ESKF, Z_0 is the estimated height in rest pose (when the foot is on the floor) and γ_z is a distance threshold. This condition represents closeness of foot to the walking floor during the stance phase. Meeting both conditions above means that the foot is both in contact with the ground and not moving. This would cancel out when the foot is in the air and undergoing very low acceleration and angular rate, as well as ignoring the cases when the foot is slipping on the floor.

Based on the dynamics of normal walking, W is chosen to represent 0.05 second ($W = 0.05/sampling freqquency$) and $\gamma_\omega = 0.01$. This is based on the assumption that foot should have an angular rate of less than $0.01 rad/s$ for at least 0.05 second, to be considered stationary. Also $\gamma_z = 0.01\ m$ was chosen to reflect the foot contact with the ground.

IV. Results

A walking test on a flat surface is presented and analyzed here. The device was attached close to the heel of the user. The test is started by 2 seconds of no-motion stance, followed by walking for 70 seconds and coming back to the initial position.

The possible measurements available to ESKF are zero velocity and foot height measurement using ToF distance sensors. The two following methods are compared:

1) ZVU
2) ZVU & ToF height correction

A. Zero Velocity Detection

The two criteria discussed in section III-C3 are presented and compared against each other in Fig. 4.

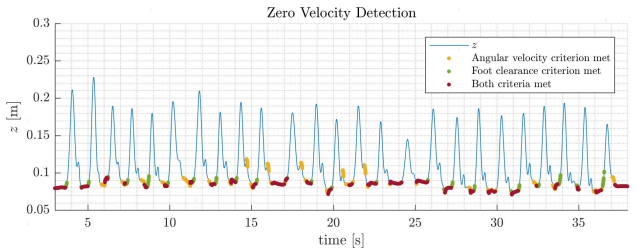

Fig. 4. Zero velocity detection using angular rate and foot height measurement

B. Comparison of Position

By comparing the start and end position one can evaluate the performance of position estimation. Other methods include comparison with optical motion tracking using cameras which is not used here. A comparison the ZVU and ZVU augmented with height measurement can be seen in Fig. 5.

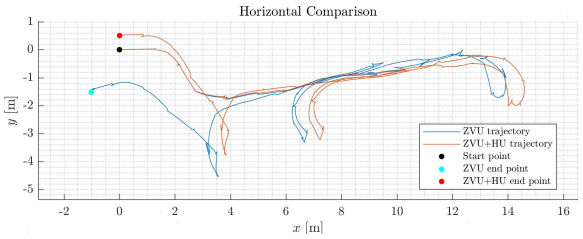

Fig. 5. Top view comparison of positioning between ZVU and ZVU+HU on the same data set corresponding to a 70 second test indoor

C. Comparison of Foot Height

Fig. 6 illustrates the ESKF foot height estimation and how it correlates with the height measurement from the distance sensor readings.

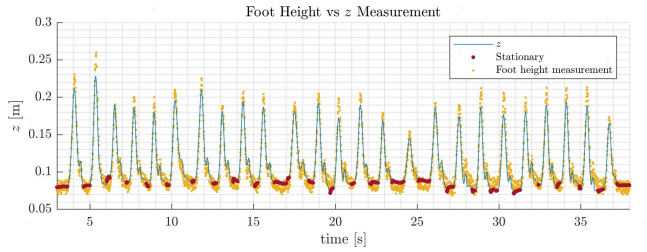

Fig. 6. Foot height estimation from ESKF and foot height measurements from the distance sensors

It can be seen that the KF closely follows the foot height measurements acquired from distance sensors, except when the foot height is maximum.

The effect of distance measurement on foot height estimation is showed in Fig. 7.

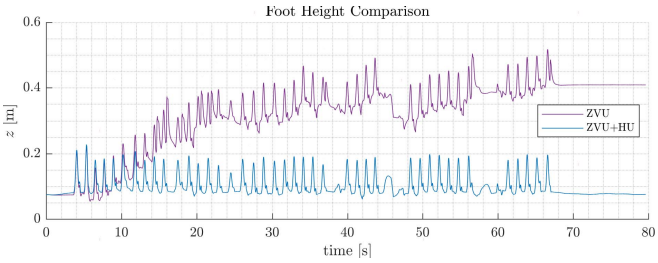

Fig. 7. Foot height comparison of ZVU vs ZVU+HU

The comparison of accumulated height error, by assuming a flat floor, is presented in Fig. 8.

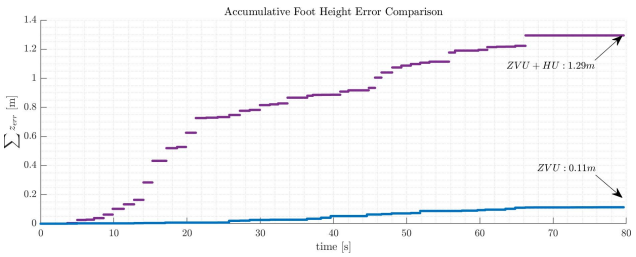

Fig. 8. Accumulative foot height error comparison of ZVU vs ZVU+HU

V. CONCLUSIONS

In this work a novel testbed for foot-mounted navigation augmented with ToF distance sensors for foot height measurement is presented. The addition of distance sensors achieves the following:

- Provides absolute foot clearance
- Significantly reduces the vertical position error during each step
- Contributes to robustness of zero velocity detection
- Increases the horizontal position accuracy due to correlation of horizontal location with vertical location through KF covariance matrix

Additionally, our system enables further study of sensor fusion algorithms.

REFERENCES

[1] P. Maillot, A. Perrot, A. Hartley, and M.-C. Do, "The braking force in walking: Age-related differences and improvement in older adults with exergame training," *Journal of aging and physical activity*, vol. 22, no. 4, pp. 518–526, 2014.

[2] E. Foxlin, "Pedestrian tracking with shoe-mounted inertial sensors," *Computer Graphics and Applications, IEEE*, vol. 25, no. 6, pp. 38–46, 2005.

[3] J.-O. Nilsson, I. Skog, and P. Hndel, "A note on the limitations of zupts and the implications on sensor error modeling," in *Proceeding of 2012 International Conference on Indoor Positioning and Indoor Navigation (IPIN), 13-15th November 2012*, Conference Proceedings, fair literature before 2012.

[4] P. D. Duong and Y. S. Suh, "Foot pose estimation using an inertial sensor unit and two distance sensors," *Sensors*, vol. 15, no. 7, pp. 15 888–15 902, 2015.

[5] A. Arami, N. Saint Raymond, and K. Aminian, "An accurate wearable foot clearance estimation system: Toward a real-time measurement system," *IEEE Sensors Journal*, vol. 17, no. 8, pp. 2542–2549, 2017.

[6] J.-O. Nilsson, I. Skog, and P. Handel, "Aligning the forceseliminating the misalignments in imu arrays," *Instrumentation and Measurement, IEEE Transactions on*, vol. 63, no. 10, pp. 2498–2500, 2014.

[7] G. Panahandeh, I. Skog, and M. Jansson, "Calibration of the accelerometer triad of an inertial measurement unit, maximum likelihood estimation and cramer-rao bound," in *Indoor Positioning and Indoor Navigation (IPIN), 2010 International Conference on*. IEEE, Conference Proceedings, pp. 1–6.

[8] A. Kozlov, I. Tarygin, and A. Golovan, "Calibration of inertial measurement units on a low-grade turntable with simultaneous estimation of temperature coefficients," in *21st Saint Petersburg International Conference on Integrated Navigation Systems*. Concern CSRI Elektropribor Saint Petersburg, Conference Proceedings, pp. 376–379.

[9] S. Stanin and S. Tomai, "Time-and computation-efficient calibration of mems 3d accelerometers and gyroscopes," *Sensors*, vol. 14, no. 8, pp. 14 885–14 915, 2014.

[10] J. Sola, "Quaternion kinematics for the error-state kalman filter," *arXiv preprint arXiv:1711.02508*, 2017.

[11] S. Bertuletti, A. Cereatti, D. Comotti, M. Caldara, and U. Della Croce, "Static and dynamic accuracy of an innovative miniaturized wearable platform for short range distance measurements for human movement applications," *Sensors*, vol. 17, no. 7, p. 1492, 2017.

[12] I. Skog, P. Handel, J.-O. Nilsson, and J. Rantakokko, "Zero-velocity detectionan algorithm evaluation," *Biomedical Engineering, IEEE Transactions on*, vol. 57, no. 11, pp. 2657–2666, 2010.